



## OPEN ACCESS

## EDITED BY

Kinga Korniejenko,  
Cracow University of Technology, Poland

## REVIEWED BY

Oleksandr Kovalchuk,  
Kyiv National University of Construction  
and Architecture, Ukraine  
Grzegorz Golewski,  
Lublin University of Technology, Poland

## \*CORRESPONDENCE

Leonid Dvorkin,  
✉ [dvorkin.leonid@gmail.com](mailto:dvorkin.leonid@gmail.com)

RECEIVED 29 March 2023

ACCEPTED 26 May 2023

PUBLISHED 07 June 2023

## CITATION

Dvorkin L and Zhitkovsky V (2023),  
Cement–ash concrete with the addition  
of lime kiln dust.

*Front. Mater.* 10:1196407.

doi: 10.3389/fmats.2023.1196407

## COPYRIGHT

© 2023 Dvorkin and Zhitkovsky. This is an open-access article distributed under the terms of the [Creative Commons Attribution License \(CC BY\)](https://creativecommons.org/licenses/by/4.0/). The use, distribution or reproduction in other forums is permitted, provided the original author(s) and the copyright owner(s) are credited and that the original publication in this journal is cited, in accordance with accepted academic practice. No use, distribution or reproduction is permitted which does not comply with these terms.

# Cement–ash concrete with the addition of lime kiln dust

Leonid Dvorkin\* and Vadim Zhitkovsky

Department Constructing Materials Technology and Material Science, Institute of Civil Engineering and Architecture, National University of Water and Environmental Engineering, Rivne, Ukraine

The article is devoted to the study of the effect of lime kiln dust (LKD) on the properties of concrete mixtures and concrete using Portland cement and fly ash. A possible mechanism for the formation of the structure of cement–ash paste with the addition of LKD is analyzed in detail. The positive effect of LKD on hydration (an increase in the content of hydration water by 40.50%) and structure formation due to an increase in the alkalinity of the cement–ash paste is shown. Using the method of the experiment mathematical planning, experimental–statistical polynomial models of the concrete component (Portland cement, fly ash, dust, superplasticizer, and aggregates) content influence on the workability of the concrete mixture and the strength of concrete at different ages were obtained. The introduction of lime–carbonate components into concrete mixtures increases the strength of concrete by 27%–54%. At the same time, with the consumption of cement up to 200 kg/m<sup>3</sup>, ash 100.150 kg/m<sup>3</sup>, and LKD 50.100 kg/m<sup>3</sup>, it seems possible to obtain concrete with a compressive strength of 20.30 MPa. The obtained models were analyzed, which made it possible to establish the positive effect of LKD additive on the compressive strength of concrete at the age of 7–180 days.

## KEYWORDS

additive, concrete, superplasticizer, ash, lime, dust

## 1 Introduction

Cement concrete is one of the most used materials in modern construction; however, due to the huge negative impact on the environment due to carbon dioxide emissions from cement production, its use is contrary to the principles of sustainable development (Golewski, 2023). One of the most effective ways to reduce the clinker component in cement concrete is the use of active mineral additives in its production (fly ash, blast furnace slag, microsilica, etc.), which can replace a certain amount of cement clinker and are also large-tonnage industrial waste (Wang et al., 2023). Reducing the amount of such waste, which, in turn, has a negative impact on the environment while in dumps, is an important task to ensure the sustainable development of society (Chinnu et al., 2021).

Lime kiln dust (LKD) is a large-tonnage waste that is generated during the production of building lime in shaft and rotary kilns and is captured in cyclones. It includes two main phases: calcium carbonate and oxide. The content of free calcium oxide in LKD is usually not less than 30%. A number of researchers have studied the effect of CaO and Ca(OH)<sub>2</sub> additives on the hydration process and cement properties (Miller and Callaghan, 2004; Hasanbeigi et al., 2012; Masimawati et al., 2015; Cao et al., 2019; Bandara et al., 2020; Wang et al., 2023). The available results are contradictory. Lamellar crystals of Ca(OH)<sub>2</sub> in certain experiments showed a positive effect on the strength of the cement stone, although in most cases the introduction of crystalline hydrates was not accompanied by an increase in the initial strength of the hardening samples. Significantly more effective than the additive

$\text{Ca}(\text{OH})_2$  was the addition of 3%–5% freshly burnt calcium oxide to the cement mortar subjected to steaming. The fact of accelerating the hardening of some types of cement, especially in combination with other accelerators, for example, with calcium chloride, with the help of calcium oxide, was noted in [Cheah et al. \(2022\)](#).

Calcium oxide and hydroxide are recommended as components of a number of patented complex hardening accelerator additives ([Ramachandran, 1995](#)). The effect of accelerating the hardening of cement by calcium oxide is explained ([Wang et al., 2018](#)) by its compensation for the so-called “lime starvation” in the early stages of cement hydration. In the experiments ([Wang et al., 2018](#)), in the liquid phase of hardening cement with  $W/C = 0.50$ , the  $\text{CaO}$  content decreased to 1 g/L after 6 h of hardening and to 0.2 g/L at the end of 3 days of age. With an artificial increase of “lime hunger” in hardening cement, the strength of the cement–sand mortar decreased 6–7 times at the age of 3 days, 2–2.5 times at 7 days, and 1.6 times at 60 days compared with the strength of the mortar on cement without removal of lime from it. Satisfying the “lime hunger” of hardening cement by adding quicklime at the rate of 2%–5% by weight of cement by 20%–40% made it possible to increase its strength.

The structure-forming role of calcium hydroxide in the hardening cement stone increases significantly with the introduction of active mineral additives. With a sufficient amount of pozzolana in cement (up to 33%), the concentration of lime in the liquid phase decreases to 2 mmol/L and lower, which corresponds to the equilibrium concentration with tobermorite phases ([Juenger et al., 2015](#)), while mixtures of Portland cement with sand have a lime concentration of more than 10 mmol/L. Active mineral additives, binding hydrolytic lime, should accelerate the hardening of cement ([Juenger et al., 2015](#)); however, under normal conditions, this effect can manifest itself in a relatively late period, provided that the water demand of mortar or concrete mixtures does not increase.

The introduction of active mineral additives into cement or concrete mixtures together with superplasticizer additives makes it possible to compensate for the increase in their water demand and significantly increase strength, and improve a number of other construction and technical properties of concrete. With an increased content of superplasticizers introduced with cement or water, it opens up the possibility of manufacturing highly filled cements of a new type—binders with low water demand. A decrease in the clinker fund in cements with an increased content and activity of the mineral filler can reduce the pH of the liquid phase of concrete below the critical limit and cause reinforcement corrosion ([Dweck et al., 2000](#)). Under these conditions, the regulation of the  $\text{Ca}(\text{OH})_2$  content in concrete due to the additional introduction of a lime additive may be appropriate and contribute to the long-term preservation of concrete performance properties, the ability to self-heal defects that occur in the structure of concrete during operation, and long-term preservation of its protective properties in relation to reinforcement.

The mechanism of the effect of  $\text{CaCO}_3$  on the processes of Portland cement curing and the formation of concrete properties has been studied in a number of works ([Poppe and De Schutter, 2005](#); [Matschei et al., 2007](#); [Zhang et al., 2023](#)). The expediency of introducing carbonate and other active additives into cements and concretes is based primarily on the well-known theoretical ideas of

V.N. Yung about cement stone as “micro-concrete.” [Matschei et al. \(2007\)](#) indicated that these materials could be added at levels of at least 10% “without fear of a drastic reduction in strength.” The chemical interaction between carbonate aggregates and hydrated cement was first established ([Wang, 2018](#)). The surface layers of carbonate aggregates were studied, and compounds were found in them, that are usually absent in the products of the reaction between cement and water. Using X-ray diffraction and differential thermal analysis, Wang (2018) discovered that calcium carbonates interact with aluminum-containing clinker minerals, forming complex compounds of the type— $3\text{C}_a\text{O} \cdot \text{Al}_2\text{O}_3 \cdot \text{CaCO}_3 \cdot 12\text{H}_2\text{O}$ . The transition of a larger amount of water into a chemically bound state contributes to a more rapid hardening of the Portland cement–additive–water system ([Wang, 2018](#)). This is especially noticeable when the clinker contains an increased amount of aluminate compounds. According to [Wang \(2018\)](#), the tensile strength of  $\text{C}_3\text{A}$ –marble and  $\text{C}_3\text{A}$ –dolomite compositions increased after 3 days and at a later age, almost 10 times compared to the strength of pure  $\text{C}_3\text{A}$ . The increase in strength  $\text{C}_4\text{AF}$  was less significant (about 10%).

In accordance with modern concepts ([Aquino et al., 2010](#)), there are two possible ways to form a hydrocarboaluminate phase in Portland cement. The first one is in the interaction of its hydration products with the carbonate filler with direct dissolution of its surface and the second one is in the interaction with lamellar hydroaluminates and calcium hydrosulfaluminates. In the second case, as a result of substitution of  $\text{Ca}(\text{OH})_2$  or  $\text{CaSO}_4$  on  $\text{CaCO}_3$ , solid hard solutions of the type  $3\text{CaO} \cdot \text{Al}_2\text{O}_3 \cdot [\text{CaCO}_3, \text{CaSO}_4, \text{Ca}(\text{OH})_2] \cdot 12\text{H}_2\text{O}$  are formed. During the hardening of real Portland cements, hydrocarboaluminates are formed after the binding of gypsum and have a more complex composition due to the partial replacement of  $\text{CaCO}_3$  by  $\text{CaSO}_4$ . Calcium hydrocarboaluminates are most intensively formed ([Wang, 2018](#)) during normal hardening of Portland cement concretes within 3–14 days from the start of hardening, i.e., their occurrence follows the decay of ettringite. Under normal conditions of hydration, the appearance of clearly distinguishable hexagonal crystals of calcium hydrocarboaluminate on the surface of calcite was recorded ([Aquino et al., 2010](#)) as early as 2–3 h after the start of hydration. During hardening in the steaming chamber, crystallization of calcium hydrocarboaluminate is fixed only at the initial stage (2.4 h of isothermal heating at  $80^\circ\text{C}$ – $90^\circ\text{C}$ ). Subsequently, the destruction of crystals is observed, due to an increase in the concentration of  $\text{CaO}$  in the liquid phase of the hardening concrete.

Along with the chemical, the physicochemical interaction of  $\text{CaCO}_3$  and hydration products has a significant effect on the formation of the hardening structure of the cement stone. Many experiments ([Bonavetti et al., 2001](#)) have shown that calcium carbonate particles in the hardening cement stone are more completely overgrown with products of hydration than of quartz. The closest structural correspondence is characteristic of calcite and hexagonal solid solutions of calcium hydroaluminate. It promotes the formation of strong bonds due to the epitaxial fusion of crystal surfaces.

Thus, the analysis of modern theoretical concepts of concrete science suggests that the introduction of a combined dispersed additive into the concrete mix, including calcium carbonate and



FIGURE 1  
Lime kiln dust (LKD).

oxide, should actively influence the processes of structure formation and formation of concrete properties. As such, a combined additive can be considered LKD. Of considerable interest is the introduction of LKD into cement–pozzolanic, for example, cement–ash systems, with a high content of mineral additives, where the structuring role of both the carbonate and lime components of the additive can be most fully used. The working hypothesis of the conducted research is that the addition of LKD to cement–ash concrete mixtures should increase the volume of hydrate products, accelerate the formation of the crystallization structure of the cement stone, and provide long-term sufficient alkalinity of the hardening concrete.

## 2 Materials and research methods

The studies were carried out on LKD, captured by cyclones during the roasting of lime in rotary kilns (Figure 1). The LKD activity in terms of CaO content was 33.6%. Its phase composition according to the results of X-ray analysis was represented by CaO—37.5%, CaCO<sub>3</sub>—47.3%, Ca(OH)<sub>2</sub>—6.8%, and 8.4%—dehydrated clay minerals. The presence of Ca(OH)<sub>2</sub> in the LKD is due to its partial slaking upon

exposure. The granulometric composition of the LKD, determined by sedimentation analysis, is as follows: <30 μm—35.4%, 30.60 μm—41.4%, 60.80 μm—15.5%, and more than 80 μm—7.7%. Concrete mixtures were made using Portland cement CEM-II/A-S of class 42.5N from the Volyn-Cement plant (Ukraine). The active mineral additive was fly ash [Burshtyn power station (Ukraine)]. The raw materials' chemical composition and specific surface area are given in Table 1.

The superplasticizer of naphthalene–formaldehyde type S-3 was introduced into concrete mixtures. In the manufacture of concrete samples, medium-sized sand with a fineness modulus of 2.0 was used as a fine aggregate, and granite-crushed stone of a fraction of 5–20 mm was used as a coarse aggregate.

The research was carried out in three stages (Figure 2). In the first stage, a cement paste was obtained, which contained various amounts of active mineral additives (lime dust and fly ash). We studied the setting time, the kinetics of changes in the plastic strength of the pastes, and the amount of hydrated water. X-ray phase and differential thermal analyses of hardened samples were carried out. In the second stage, a concrete mixture was obtained, on which the influence of the composition of concrete and active mineral additives on water demand and workability, as well as the compressive strength of concrete cubes 100\*100\*100 mm, was determined. The experiment was carried out according to the mathematical plan. A total of 360 samples were manufactured, 288 samples were hardened under normal conditions, and 72 samples were cured in a steaming chamber at a temperature of 80°C (Figure 3). In the third stage of the research, statistical data processing was carried out, and experimental–statistical models of the concrete mixture water demand and workability, as well as the compressive strength of concrete under normal conditions and during steaming, were obtained.

The processes of hydration and structure formation in the cement–ash–LKD system, as well as the properties of cement–ash concrete mixtures with the addition of LKD and concretes based on them, were studied using structural parameters characterizing the volume concentration:

LKD in ash–lime additive:

$$X_1 = V_{LKD} / (V_{LKD} + V_{ash}). \quad (1)$$

Ash–lime additive in a composite binder:

$$X_2 = (V_{LKD} + V_{ash}) / (V_{LKD} + V_{ash} + V_c). \quad (2)$$

Composite binder in cement–ash–lime LKD paste:

$$X_3 = (V_{LKD} + V_{ash} + V_c) / (V_{LKD} + V_{ash} + V_c + V_w). \quad (3)$$

Dry superplasticizer in a water solution:

TABLE 1 Raw material characteristics.

| Material        | Chemical composition, % |                                |                                |       |      |                 |                   |          | Specific surface area, m <sup>2</sup> /kg |
|-----------------|-------------------------|--------------------------------|--------------------------------|-------|------|-----------------|-------------------|----------|---|
|                 | SiO <sub>2</sub>        | Al <sub>2</sub> O <sub>3</sub> | Fe <sub>2</sub> O <sub>3</sub> | CaO   | MgO  | SO <sub>3</sub> | R <sub>2</sub> O* | L.O.I.** |   |
| Portland cement | 21.80                   | 5.12                           | 4.11                           | 65.80 | 0.95 | 0.63            | 0.85              | 0.81     | 340                                       |
| Fly ash         | 53.5                    | 21.4                           | 10.8                           | 3.24  | 1.35 | 2.32            | —                 | 8.2      | 320                                       |
| LKD             | 7.2                     | 1.0                            | 0.2                            | 69.12 | 0.25 | —               | —                 | 22.23    | 380                                       |

\*R<sub>2</sub>O = Na<sub>2</sub>O + K<sub>2</sub>O, \*\*L.O.I, loss on ignition.

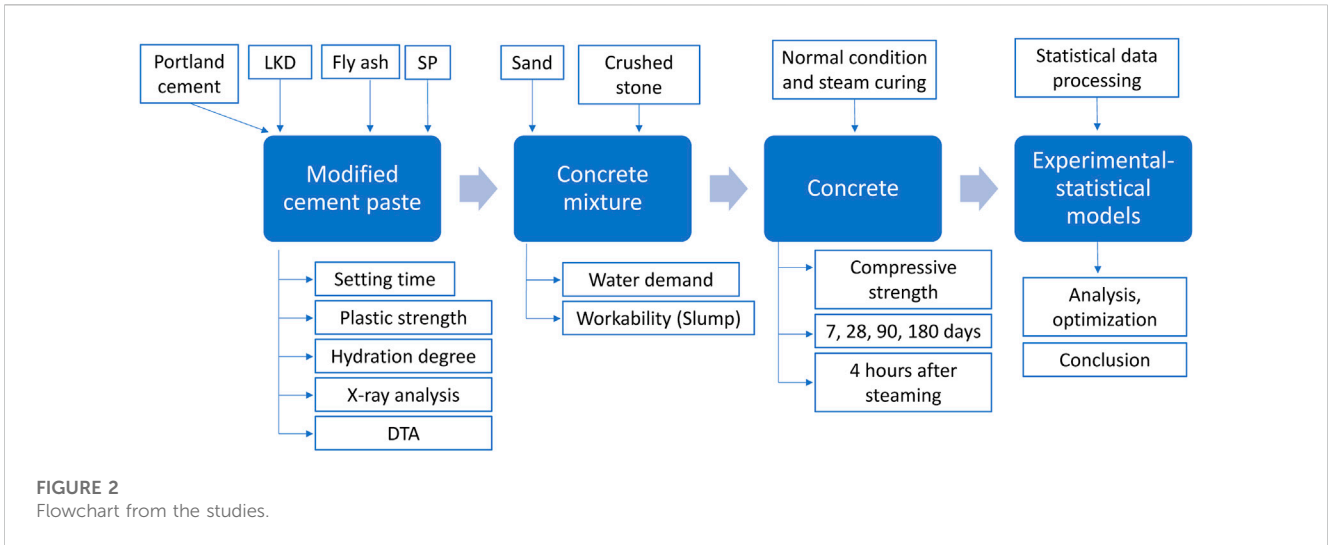


FIGURE 2 Flowchart from the studies.



FIGURE 3 Study of cement paste hydration: (A) cube sample 20 × 20 × 20 mm and mold; (B) sample after grinding and muffle furnace.

$$X_{SP} = V_{SP} / (V_{SP} + V_w). \tag{4}$$

In equations (1)–(4),  $V_{LKD}$ ,  $V_{ash}$ ,  $V_c$ ,  $V_w$ , and  $V_{SP}$  are, respectively, the volume consumptions of LKD, fly ash, Portland cement, water, and superplasticizer for cement–ash–lime pastes.

The mass consumption of these materials can be found taking into account the density values of the initial materials ( $\rho_{LKD} = 2.5 \text{ g/cm}^3$ ,  $\rho_{ash} = 2.4 \text{ g/cm}^3$ ,  $\rho_c = 3.1 \text{ g/cm}^3$ ,  $\rho_w = 1 \text{ g/cm}^3$ , and  $\rho_{SP} = 1.168 \text{ g/cm}^3$ ).

Along with the parameters  $X_1 \dots X_3$  discussed previously, characterizing the structure and composition of the cement paste with additives, was introduced an additional parameter  $X_4$ , which characterizes its volume concentration in the concrete mix

$$X_4 = (V_{LKD} + V_{ash} + V_c + V_w) / (V_{LKD} + V_{ash} + V_w + V_{ag}), \tag{5}$$

where  $V_{ag}$  is the volume consumption of the aggregate.

When calculating the amount of the hydration water, we subtracted the amount of water used to convert the CaO contained in the LKD to  $\text{Ca(OH)}_2$ . The intensity of the cement

paste hydration was studied by determining the amount of chemically bound water in % of the mass of cement both at normal temperature and during steaming. For this purpose, cube samples  $20 \times 20 \times 20 \text{ mm}$  in size were made, which were crushed at a given age, treated with acetone, then dried at  $105^\circ\text{C}$ , and calcined at  $1000^\circ\text{C}$  (Figure 3). The amount of chemically bound water was determined by the difference in weight during calcination and drying (Zhao and Khoshnazar, 2021). The study of the process of early structure formation of cement pastes was carried out by measuring the kinetics of changes in plastic strength with a Rebinder cone (Dvorkin et al., 2022).

To obtain comparative results, ground quicklime was introduced into cement–ash pastes. The technological properties of concrete mixtures and the strength of cement–ash concrete with LKD addition were studied using the methodology of experiment planning, with the help of which the necessary experimental and statistical models were obtained (Box, 2005; CEN:2009; CEN:2021). Samples were made and tested according to standard methods (CEN:2009; CEN:2021) (Figure 4).



**FIGURE 4** Concrete samples with LKD and their testing: **(A)** normal hardening chamber; **(B)** sample before and after determination of compressive strength.

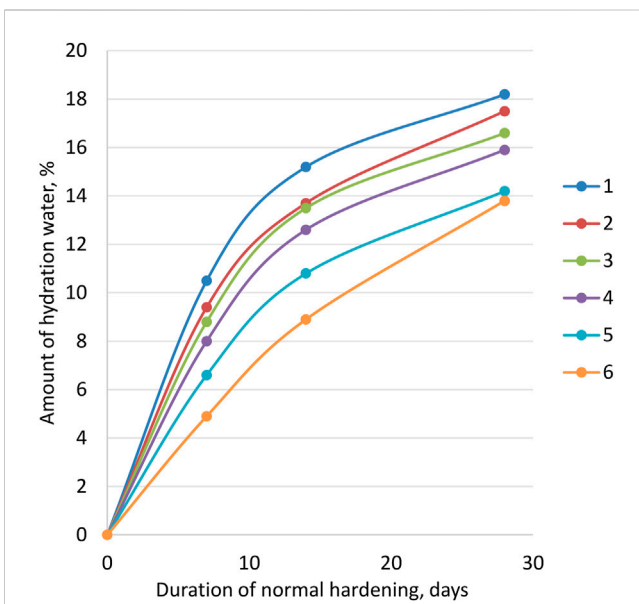


**FIGURE 5** Hydration intensity of cement pastes:  
 1—cement—ash—lime—carbonate paste:  $X_1 = 0,6$ ;  $X_2 = 0,6$ ;  $X_3 = 0,4$ ;  
 2— $X_1 = 0,4$ ;  $X_2 = 0,5$ ;  $X_3 = 0,4$ ; 3— $X_1 = 0,4$ ;  $X_2 = 0,4$ ;  $X_3 = 0,4$ ;  
 4—cement—ash paste with the addition of ground quicklime (CaO = 5%); 5—cement—ash paste. **Note:**  $X_1 = V_{LKD} / (V_{LKD} + V_{ash})$ ,  
 $X_2 = (V_{LKD} + V_{ash}) / (V_{LKD} + V_{ash} + V_c)$ ,  
 and  $X_3 = (V_{LKD} + V_{ash} + V_c) / (V_{LKD} + V_{ash} + V_c + V_w)$ .

When choosing the area of factor variation, the task was to cover a fairly wide range of compositions of concrete mixes—from low-slump to cast with reduced and moderate cement consumption.

When setting up experiments, the composition of concrete mixtures at each point of the matrix was calculated using the following formulas:

$$\begin{aligned}
 LKD &= X_1 X_2 X_3 X_4 \rho_{LKD}; & AG &= (1 - X_1) X_2 X_3 X_4 \rho_{ash}, \\
 C &= (1 - X_2) X_3 X_4 \rho_c; & V &= (1 - X_3) X_4 \rho_w; \\
 AG &= (1 - X_4) \rho_{AG}, & &
 \end{aligned}
 \tag{6}$$

where  $\rho_{LKD}$ ,  $\rho_{ash}$ ,  $\rho_c$ ,  $\rho_w$ , and  $\rho_{AG}$  are densities, respectively, of LKD, ash, cement, water, and aggregates ( $\rho_{LKD} = 2,4$ ;  $\rho_{ash} = 2,2$ ;  $\rho_c = 3,1$ ;  $\rho_w = 1$ ;  $\rho_{AG} = 2,65 \text{ g/cm}^3$ ).

LKD consumption varied within  $52.164 \text{ kg/m}^3$ ; ash— $99.257$ ; cement— $133.325$ ; water— $164.265 \text{ kg/m}^3$ .

### 3 Experimental results

**Hydration and structure formation of cement—ash—lime—carbonate pastes.** The results of experiments to determine the intensity of the paste hydration of the studied compositions are shown in Figure 5.

Analysis of the data obtained for pastes of various compositions shows that the transition from cement—ash pastes to cement—ash—lime—carbonate pastes increases the amount of the hydration water in 7 days of normal hardening by 30.50%, and in 28 days by 20.40%. In the studied pastes, the content of LKD varied by weight from 15% to 50% of the mass of the cement—ash part. The ash content varied from 40% to 60% of the mass of cement. Characteristically, with almost the same additional amount of CaO, due to the introduction of LKD and quicklime, in the first case, a higher intensity of hydration is provided, especially

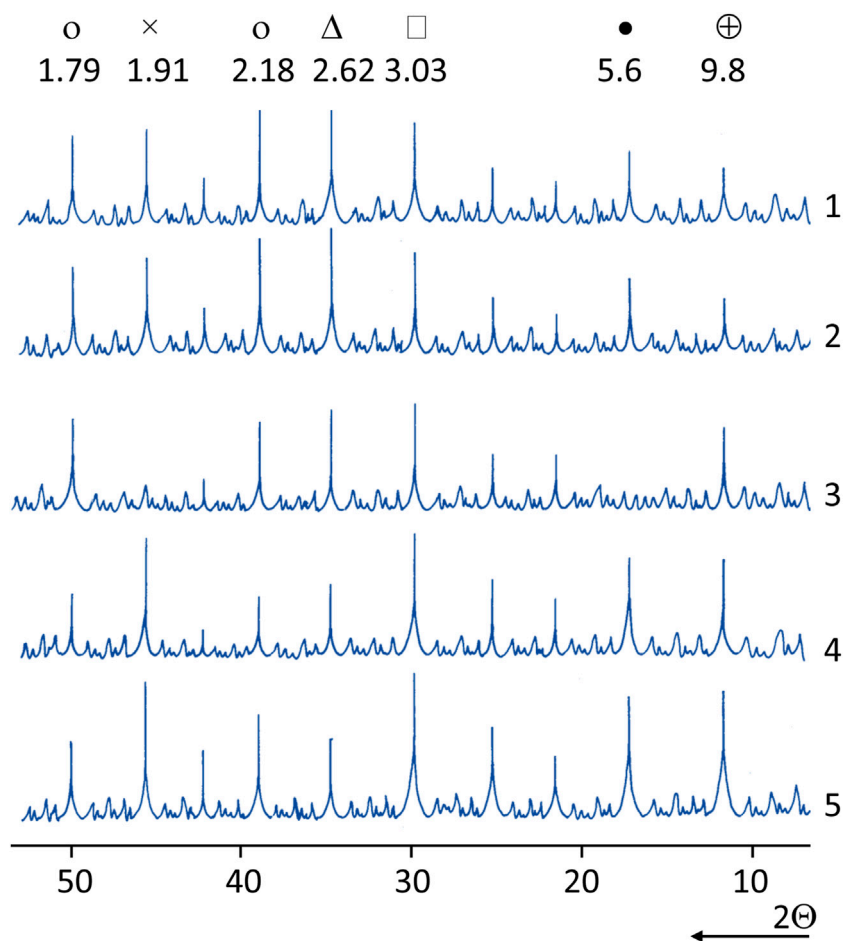


FIGURE 6

X-ray patterns of the normal hardening cement and cement-ash paste with LKD: 1–cement paste: 1–LKD–15% of the cement mass; 2–LKD–20%; 3–5–cement-ash paste (fly ash–40%): 3–CaO = 5%; 4–LKD = 15%; 5–LKD = 20% (o–portlandite; Δ–alite; □–CSH(O) hydrosilicates; ●–ettringite; x–calcite; ⊕–hydrocarboaluminate).

noticeable at 28 days, which can be explained by the catalytic effect of calcium carbonate.

More intensive hydration of cement-ash systems with additives of LKD is confirmed by differential thermal (DTA) and X-ray analyses. The introduction of LKD into both cement and, especially, cement-ash pastes increases the magnitude of the endothermic effects of the decomposition of hydrate products. The thermograms also show slight exothermic effects at 900°–960°C, due to the recrystallization of calcium hydrosilicate dehydration products. On the X-ray diffraction patterns (Figure 6) of the studied samples, an increase in the intensity of the analytical lines, characteristic of the hydration products of cement and ash in the presence of LKD additives, is noticeable. For samples of cement-ash stone without the addition of LKD, stronger lines ( $d = 3.03$ ;  $3.07$ ) of hydrosilicates of the CSH(B) type appear after steaming and at 28 days. Accordingly, the intensity of the lines of alite ( $d = 2.62$ ;  $1.79$ ) and portlandite ( $d = 2.62$ ;  $1.79$ ) decreases.

In samples with the addition of LKD, the identification of hydrosilicates is hampered by the practical coincidence of the interplanar distance of their strongest analytical line ( $d = 3.07$ ) with the strongest calcite line ( $d = 3.03$ ).

In steamed samples of cement-ash stone without the addition of LKD and in samples of 28-day normal hardening, the hydrosulfoaluminate phase is represented by the monosulfate form of hydrosulfoaluminate ( $d = 8.9$ ;  $4.5$ ), and in other compositions by ettringite ( $d = 9.8$ ;  $5.6$ ).

For samples of cement and cement-ash stone with the addition of LKD in 28 days, normal hardening recorded the strongest analytical lines of the hydrocarboaluminate phase ( $d = 7.71$ ;  $3.78$ ). The absence of the hydrocarboaluminate phase in the steamed samples is consistent with the well-known data (Matschei et al., 2007) on its destruction during steaming for more than 4 h as the liquid phase of the hardening stone is saturated with CaO.

The active influence of LKD on the rheological properties and hydration rate of cement-ash pastes and its chemical and physico-chemical interaction with cement and ash should also affect the formation of both coagulation and crystallization structures of cement-ash stone. The formation of the coagulation structure of cement pastes is completed, as is known, by the end of their setting. If fly ash lengthens the setting time, then the introduction of LKD leads to a reduction in the setting time of cement and cement-ash

TABLE 2 Influence of LKD on the paste setting time.

| Structural parameters |                | Composition of dry pastes by volume |                  |                | Setting time, hour-min |       |
|-----------------------|----------------|-------------------------------------|------------------|----------------|------------------------|-------|
| X <sub>1</sub>        | X <sub>2</sub> | V <sub>LKD</sub>                    | V <sub>ash</sub> | V <sub>c</sub> | Initial                | Final |
| —                     | —              | —                                   | —                | 1              | 2-40                   | 4-50  |
| —                     | —              | —                                   | 0.5              | 0.5            | 3-30                   | 5-40  |
| —                     | —              | 0.1                                 | —                | 0.9            | 1-50                   | 4-30  |
| —                     | —              | 0.2                                 | —                | 0.8            | 1-30                   | 4-05  |
| 0.4                   | 0.4            | 0.16                                | 0.24             | 0.6            | 2-30                   | 4-50  |
| 0.4                   | 0.5            | 0.2                                 | 0.3              | 0.5            | 2-10                   | 4-20  |
| 0.5                   | 0.6            | 0.3                                 | 0.5              | 0.3            | 2-50                   | 4-40  |
| 0.5                   | 0.4            | 0.2                                 | 0.2              | 0.6            | 1-50                   | 4-20  |
| 0.5                   | 0.5            | 0.25                                | 0.25             | 0.5            | 1-40                   | 4-10  |
| 0.5                   | 0.6            | 0.3                                 | 0.3              | 0.4            | 1-50                   | 3-50  |
| 0.6                   | 0.4            | 0.24                                | 0.16             | 0.6            | 1-30                   | 3-40  |
| 0.6                   | 0.5            | 0.3                                 | 0.2              | 0.5            | 1-20                   | 3-40  |
| 0.6                   | 0.6            | 0.36                                | 0.24             | 0.4            | 1-15                   | 3-30  |

$X_1 = V_{LKD} / (V_{LKD} + V_{ash})$  and  $X_2 = (V_{LKD} + V_{ash}) / (V_{LKD} + V_{ash} + V_c)$ .

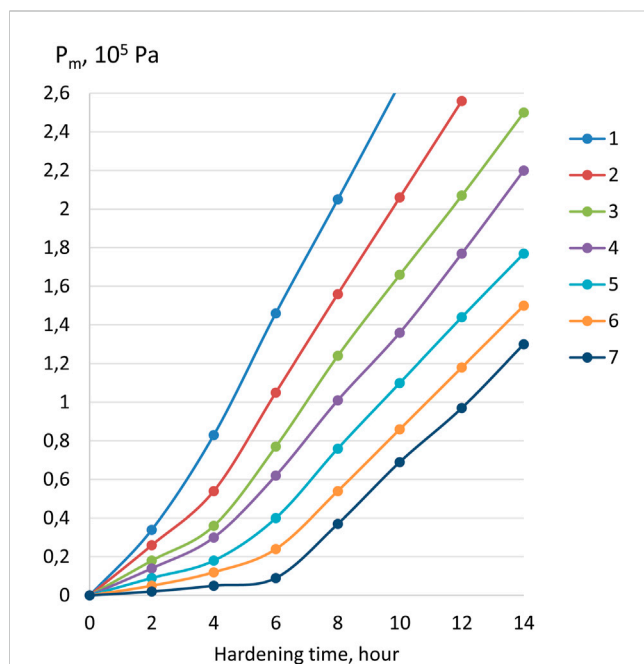


FIGURE 7 Influence of the LKD additive on the plastic strength ( $P_m$ , Pa) of the normal consistency pastes: 1— $X_1 = 0,6; X_2 = 0,4; X_{sp} = 0,02$ ; 2— $X_1 = 0,6; X_2 = 0,4; X_{sp} = 0$ ; 3— $X_1 = 0,4; X_2 = 0,4; X_{sp} = 0,02$ ; 4— $X_1 = 0,4; X_2 = 0,4; X_{sp} = 0$ ; 5—cement-ash paste with an ash content of 40% of the mass of cement and the addition of ground quicklime (CaO = 5%); 6—cement-ash paste (40% ash); 7—cement paste. Note:  $X_1 = V_{LKD} / (V_{LKD} + V_{ash})$ ,  $X_2 = (V_{LKD} + V_{ash}) / (V_{LKD} + V_{ash} + V_c)$ , and  $X_{sp} = V_{sp} / (V_{sp} + V_w)$ .

pastes (Table 2). The acceleration of setting due to LKD can be explained by an increase in the volume of hydration products, with a corresponding decrease in the distance between particles and the appearance of cohesive forces proportional to the number of particles in contact with each other.

An increase in the strength of coagulation contacts of cement-ash pastes with the introduction of LKD follows from the analysis of plastograms obtained by measuring plastic strength with a Rebinder cone (Figure 7). Attention is drawn to the significant influence of the LKD in the second section of the plastograms, corresponding to the period of hardening of the coagulation and the beginning of the formation of the crystallization structure. The steeper slope of the curve for a paste with LKD compared to the curve for a paste containing ordinary ground quicklime with an approximately equal content of ash and CaO in both pastes confirms the active role of the carbonate filler of LKD in the formation of the coagulation-crystallization structure of cement-ash stone. The structuring effect of LKD increases with a decrease in the normal consistency of pastes due to the introduction of a superplasticizer additive. This can be explained by the creation of “constrained” conditions in hardening systems under which, with an increase in the concentration of the solid phase, interparticle contact increases, and the role of dispersed fillers as “seeds” of crystallization of hydrate products increases.

**Water demand and slump of the concrete mixtures.** The influence of the composition of binders on the water demand of concrete mixtures was studied with a change in the parameters  $X_1$  and  $X_2$ , which characterize the volume concentration of LKD in the carbonate-ash part of the binder and the total volume of LKD and

TABLE 3 Water demand of concrete mixes, kg/m<sup>3</sup>.

| $X_2 = (V_{LKD} + V_{ash}) / (V_{LKD} + V_{ash} + V_{sp})$ | $X_1 = V_{LKD} / (V_{LKD} + V_{ash})$ |             |             |             |             |
|--|---------------------------------------|-------------|-------------|-------------|-------------|
|  | $X_1 = 0$                             | $X_1 = 0,1$ | $X_1 = 0,2$ | $X_1 = 0,4$ | $X_1 = 0,6$ |
| Sl = 16–18 cm  |                                       |             |             |             |             |
| 0.4  | 190/165                               | 195/165     | 205/170     | 220/180     | 240/195     |
| 0.6  | 195/170                               | 205/175     | 215/180     | 230/190     | 250/210     |
| Sl = 10–15 cm  |                                       |             |             |             |             |
| 0.4  | 180/155                               | 185/160     | 200/165     | 210/170     | 225/185     |
| 0.6  | 185/160                               | 195/165     | 210/170     | 220/180     | 230/200     |
| Sl = 5–7 cm  |                                       |             |             |             |             |
| 0.4  | 170/150                               | 180/155     | 190/160     | 200/170     | 215/180     |
| 0.6  | 175/155                               | 185/160     | 195/165     | 210/175     | 220/190     |
| Sl = 1–3 cm  |                                       |             |             |             |             |
| 0.4  | 165/145                               | 170/150     | 180/155     | 190/165     | 205/170     |
| 0.6  | 175/150                               | 180/155     | 190/160     | 200/170     | 210/185     |

Below the line is the water demand of mixtures with the superplasticizer.

ash in the volume of the binder, respectively. The consumption of cement was assumed to be constant and equal to 150 kg/m<sup>3</sup> ( $V_{sp} = 0.048 \text{ m}^3$ ).

Experimental values of water demand for concrete mixes containing LKD at various indicators of workability are given in Table 3.

An increase in the values of both  $X_1$  and  $X_2$ , which determine, respectively, the portion of LKD in the composition of the non-cement part of the binder and its content in concrete mixtures in all studied compositions without the addition of a superplasticizer, causes an increase in water demand. Concrete mixtures with  $X_1 = 0.1$  have a water demand of 2.6.5.7% more than with  $X_1 = 0$ , with  $X_1 = 0.2$  by 7.9.11.7%, and with  $X_1 = 0.6$  by 24.2.28.2%. At the same time, the transition from  $X_2 = 0.4$  to  $X_2 = 0.6$  causes an additional increase in water demand by 2.5%.

A more significant increase in water demand with an increase in  $X_1$  is noted (Table 3) as the slump of concrete mixtures increases. So, for mixtures with Sl = 16.20 cm, an increase in  $X_1$  from 0 to 0.6 causes an increase in water demand by 50.55 L, while for sedentary mixtures with Sl = 1.4 cm, it is only 35.40 L.

By introducing a superplasticizer, it is possible to largely level out the difference in the water demand of mixtures containing LKD and without it, especially at moderate  $X_1$  values. Thus, at  $X_1 = 0.2$ , the introduction of superplasticizer S-3 makes it possible to provide the necessary slump for all compositions of mixtures at a water consumption of only 5–10 L more than in compositions without LKD. Without superplasticizers, the increase in water demand is 15–20 L.

The plasticizing effect of the superplasticizer is most pronounced as the initial water content increases. In cast mixtures without LKD, the addition of superplasticizer S-3 makes it possible to reduce water consumption by 25 L, with

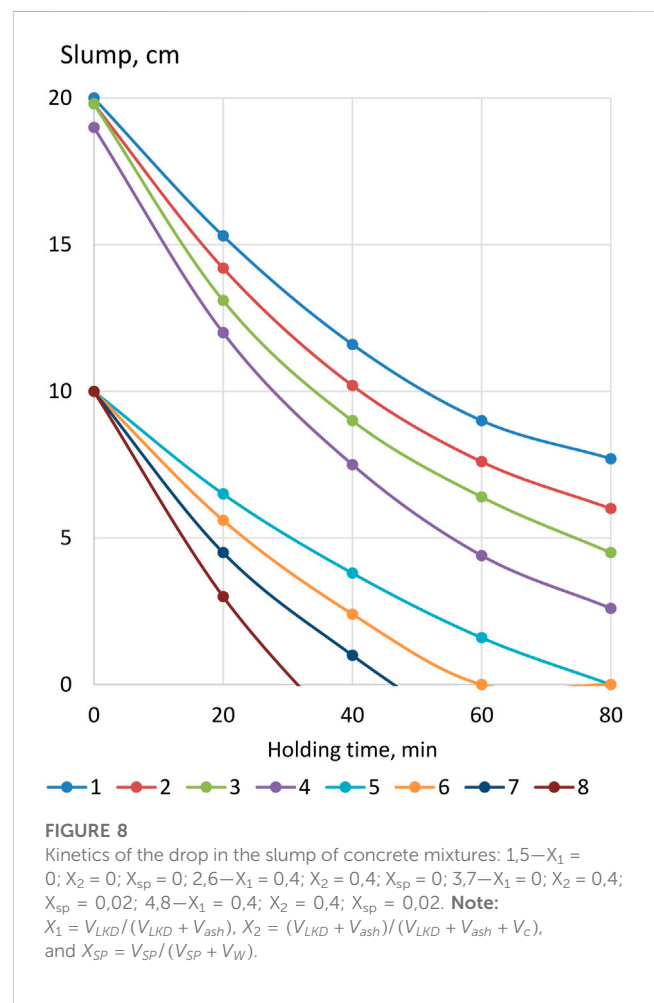




TABLE 4 Conditions for planning experiments in the study of the workability and concrete mixture strength of.

| Factors        | Levels of variation |      |      | Interval variations |
|----------------|---------------------|------|------|---------------------|
|                | −1                  | 0    | +1   |                     |
| X <sub>1</sub> | 0.3                 | 0.37 | 0.44 | 0.07                |
| X <sub>2</sub> | 0.56                | 0.63 | 0.70 | 0.07                |
| X <sub>3</sub> | 0.41                | 0.47 | 0.53 | 0.06                |
| X <sub>4</sub> | 0.35                | 0.4  | 0.45 | 0.05                |

$$X_1 = V_{LKD}/(V_{LKD} + V_{ash}), X_2 = (V_{LKD} + V_{ash})/(V_{LKD} + V_{ash} + V_c), X_3 = (V_{LKD} + V_{ash} + V_c)/(V_{LKD} + V_{ash} + V_c + V_w), X_4 = (V_{LKD} + V_{ash} + V_c + V_w)/(V_{LKD} + V_{ash} + V_w + V_{ag}).$$

LKD at X<sub>1</sub> = 0.2 by 35 L and at X<sub>1</sub> = 0.6 per 45 L. In slow-moving mixtures, the reduction in water demand is 20, 25, and 35 L, respectively.

As is known, the slump of concrete mixtures, especially with the addition of a superplasticizer, rapidly decreases during their curing and, accordingly, the water demand increases (Mailvaganam and Rixom, 2019). Figure 8 shows data characterizing the kinetics of the slump loss of various compositions of concrete mixtures over time at normal temperature. The slump of cast mixtures without LKD and S-3 additives after 30 min decreases by about 5 cm, and with the addition of S-3 by 7 cm, which is consistent with the data of other studies (Dvorkin and Dvorkin, 2006). A more intense rate of decline in the slump of concrete mixtures containing superplasticizers is naturally explained by their lower water content and, accordingly, lower W/C. The value of the latter, as is known, significantly affects the rate of hydration and structure formation of cement stone. According to Locher (2006), in cement with a strength of 37.5 MPa at W/C = 0.4, the first contacts between hydrate products are established after hydration of 18% of its grains, at W/C = 0.6—after 50%, and with W/C = 0.8—even 80%.

Superplasticizer additives, like other surfactant additives, form adsorption layers on the surface of cement particles; however, these layers are permeable, and after some initial slowdown, hydration accelerates, which contributes to the thickening of the concrete mixture (Dvorkin et al., 2023).

Mixtures with LKD lose their slump somewhat faster than without it, which is consistent with the change in the setting time and plastic strength of the cement–ash paste. At the same time, the acceleration of the rate of decline in the slump of concrete mixtures under the influence of LKD is relatively small and less noticeable than in concrete mixtures with the addition of a superplasticizer.

To study the influence of the totality of factors of the composition of concrete mixtures filled with ash and LKD, on their workability, algorithmic experiments were carried out in accordance with a typical three-level plan (Dvorkin et al., 2012). The conditions for planning experiments are given in Table 4.

Statistical processing of the obtained experimental data made it possible to obtain a polynomial mathematical model of the workability of concrete mixtures (slump) of the studied compositions at a 95% probability level:

$$Y_{sl} = 6.5 - 2.4X_1 - 1.5X_2 + 2.9X_4 - 1.1X_1^2 - 0.7X_2^2 - 0.5X_2^2 + 0.7X_1X_2 - 1.4X_2X_4. \quad (7)$$

Analysis of the model (Figure 9) shows that the change in the parameters X<sub>1</sub> and X<sub>2</sub> of the region of variation has an unequal effect on the magnitude of the concrete mix slump. The most intense decrease in the slump takes place with an increase in X<sub>1</sub> from 0.3 to 0.37, respectively, and a decrease in X<sub>4</sub> from 0.45 to 0.4, i.e., in the first half of the area of variation of factors. A significant effect of the interaction of factors X<sub>1</sub> and X<sub>2</sub> shows that a simultaneous increase in the value of these factors or their decrease enhances their integral effect. There is also a significant interaction between factors X<sub>2</sub> and X<sub>4</sub>. The effect of the interaction of these factors leads to a decrease in the slump with their multidirectional change.

In the obtained polynomial regression equation for the concrete mixture slump, the influence of the X<sub>3</sub> factor turned out to be insignificant. This factor can be interpreted as the concentration of the solid phase volume in the paste volume, i.e., in essence, the density of the paste. It is known from concrete technology that up to a certain critical C/W—a parameter also proportional to the density of the cement paste—the rule of the water demand constancy is maintained, i.e., with a change in C/W, the slump practically remains constant (Dvorkin and Dvorkin, 2006). Obviously, in this case, for concrete mixes with fly ash additive and the additive of the LKD, the rule of the water demand constancy is also preserved, while, along with the volume of the filled paste, significantly affect slump both the concentration of LKD and the concentration of the ash–carbonate–lime part in the solid phase of the paste contained in concrete mixes.

**The concrete strength.** Lime kiln dust, actively participating in the processes of hydration and structure formation, has a positive effect on the strength of cement–ash pastes, especially with the simultaneous action of a superplasticizer. To assess the effect of LKD on the strength of cement–ash concrete, a series of experiments was carried out in accordance with the five-factor plan (Dvorkin et al., 2012) and the conditions for variation factors (Table 4). The initial materials in the manufacture of samples were taken the same as in the determination of concrete mixture slump. Factors X<sub>1</sub> and X<sub>4</sub> varied in the same area as in the study of slump. In addition, the influence of the X<sub>sp</sub> factor was also studied—the concentration of the superplasticizer S-3 in the mix with water (X<sub>sp</sub> = V<sub>sp</sub>/(V<sub>sp</sub> + V<sub>w</sub>), where V<sub>sp</sub> is the absolute volume of dry matter S-3 and V<sub>w</sub> is the volume of mixing water). Factor X<sub>sp</sub> varied in the range: 0.01 ± 0.01.

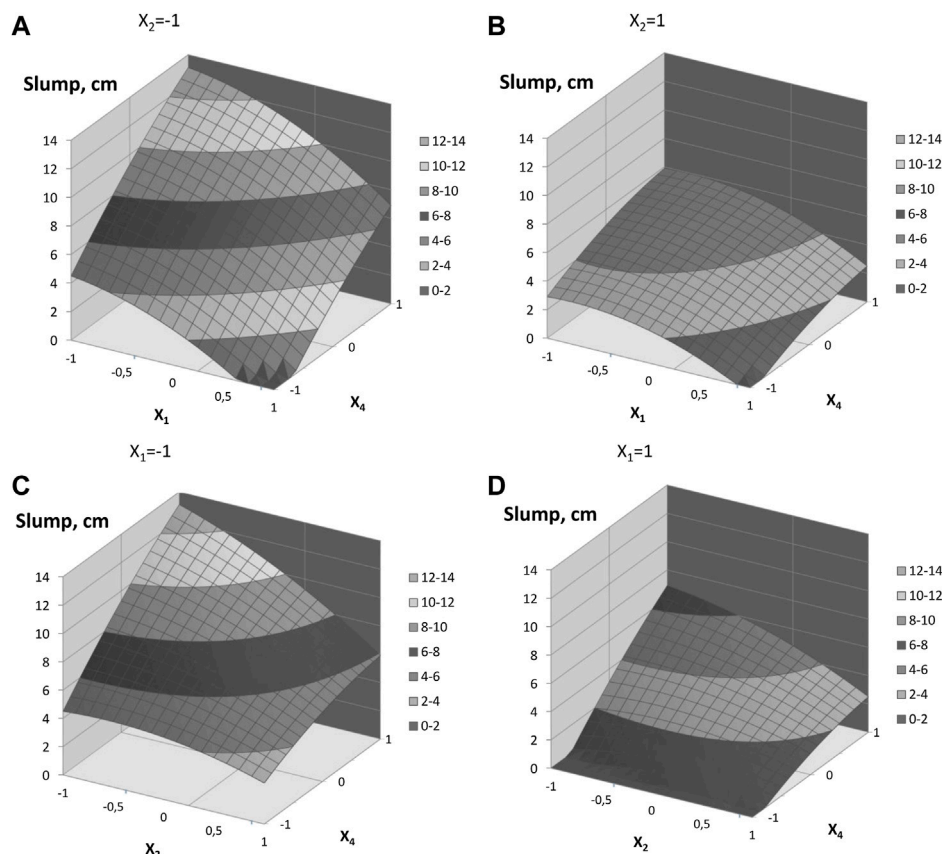


**FIGURE 9** Response surfaces of the concrete mixture slump: (A), (B)—influence of factors  $X_1$  and  $X_4$ ; (C), (D)—influence of factors  $X_2$  and  $X_4$ . **Note:**  $X_1 = V_{LKD} / (V_{LKD} + V_{ash})$ ,  $X_2 = (V_{LKD} + V_{ash}) / (V_{LKD} + V_{ash} + V_c)$ , and  $X_4 = (V_{LKD} + V_{ash} + V_c + V_w) / (V_{LKD} + V_{ash} + V_w + V_{ag})$ .

The strength of concrete samples was determined after 28 days of normal hardening ( $R_{28}$ ) and 4 h after steaming ( $R_{st}$ ). Steaming of cube samples  $100 \times 100 \times 100$  mm was carried out according to the mode 2) + 3 + 6+2 at  $80^\circ\text{C}$ .

Statistical processing of experimental data made it possible to obtain the corresponding mathematical models of concrete strength, given as follows in coded values of variables:

$$Y_{R28} = 28.5 + 5.5X_1 - 5.8X_2 + 4.7X_3 + 1.9X_{sp} - 1.8X_1^2 - 0.5X_2^2 - 0.2X_3^2 - 0.6X_{sp}^2 - 1.2X_1X_{sp} + 1.1X_1X_2, \quad (8)$$

$$Y_{Rst} = 21.5 + 4.4X_1 - 4.3X_2 + 3.4X_3 + 1.05X_c - 1.3X_1^2 - 0.3X_2^2 - 0.15X_3^2 - 0.5X_{sp}^2 - 0.8X_1X_{sp} + 0.7X_1X_2. \quad (9)$$

An analysis of the models (Tables 5; Table 6) shows that an increase in the share of LKD in the composition of the binder— $X_1$  up to a certain limit, as well as the ratio of LSD and fly ash at close values of the cement–water ratio—leads to a noticeable increase in the strength of concrete. So, at  $X_1 = 0.3$  and  $\text{LKD}/3 = 0.46$ , the strength of concrete increases (Table 5) compared to concrete without LKD from 15 to 19 MPa, i.e., by 26.6%. With an increase in  $X_1$  to 0.37 and  $\text{LKD}/3$  to 0.56, the strength further increases to 24.5 MPa, i.e., by 28.9%. With a further increase in  $X_1$  to 0.44 and  $\text{LKD}/$

$3 = 0.85$ , the increase in concrete strength slows down and is already 13.3%. Increasing the LKD content by more than  $100 \text{ kg}/\text{m}^3$  is inexpedient. Thus, at the consumption of  $\text{LKD} = 112 \text{ kg}$  and  $\text{LKD}/3 = 0.46$ , the design strength of concrete is 23% lower than with the LKD content of  $52 \text{ kg}/\text{m}^3$  and the same lime–ash ratio. In addition, with an excessively high content of LKD, the water demand of concrete mixtures sharply increases, at a constant value of  $X_1$ , but with an increase in  $X_2$ , the strength decreases, which can be explained by a corresponding decrease in  $C/W$ . Thus, at  $X_1 = 0.44$ , the increase in  $X_2$ , i.e., the concentration of the lime–carbonate–ash part in the volume of the binder from 0.56 to 0.70, leads to a decrease in  $C/W$  from 0.95 to 0.64 and a corresponding decrease in strength from 27.8 to 20.8 MPa.

With an increased value of  $X_2$ , the cement–water ratio and, accordingly, the strength of concrete can be maintained and even increased by increasing the value of the  $X_3$  parameter—i.e., volume concentration of solid components— $(V_{LKD} + V_{ash} + V_c)$  in the total volume of the binder— $(V_{LKD} + V_{ash} + V_c + V_w)$ . Cement–ash concretes in the studied range of compositions make it possible to provide compressive strength from 10 to 26 MPa at the 28-day age of normal hardening (Table 5). The introduction of lime–carbonate

**TABLE 5 Slump and strength of cement–ash concrete without the addition of LKD.**

| Consumption of materials, kg/m <sup>3</sup> |           |          | Slump, cm | Compressive strength, MPa |                                       |
|---|-----------|----------|-----------|---------------------------|---------------------------------------|
| Ash A)                                      | Cement C) | Water W) |           | Normal hardening concrete | Steamed concrete (4 h after steaming) |
| 113   | 174       | 189      | 10/24     | 15/14.5                   | 9.7/9.3                               |
| 101   | 174       | 189      | 10/24     | 15.5/14                   | 9.5/8.8                               |
| 90  | 179       | 189      | 10/24     | 15.7/14.5                 | 10.4/10.7                             |
| 114   | 122       | 189      | 2/24      | 10.2/11.5                 | 7.2/7.6                               |
| 146   | 158       | 150      | 2/12      | 12.5/12                   | 8.2/7.8                               |
| 192   | 207       | 197      | 14/24     | 18.6/165                  | 12.9/12.3                             |
| 240   | 207       | 197      | 14/24     | 17.5/18                   | 11.3/11.8                             |
| 152   | 199       | 196      | 14/24     | 15.4/14.5                 | 10.8/10.1                             |
| 117   | 231       | 150      | 1/12      | 26.5/27.5                 | 18.5/18.8                             |

Above the line is shown the slump and the strength of concrete without the addition of S-3, and below the line that with the addition of S-3 at  $X_{sp} = 0.02$ .

**TABLE 6 Slump and strength of cement–ash concretes with LKD addition.**

| Composition parameters |                |                |                | Sl, cm | Consumption of materials, kg/m <sup>3</sup> |     |     |     | Compressive strength in 28 days, MPa |
|------------------------|----------------|----------------|----------------|--------|---|-----|-----|-----|--------------------------------------|
| X <sub>1</sub>         | X <sub>2</sub> | X <sub>3</sub> | X <sub>4</sub> |        | LKD   | Ash | C   | W   |                                      |
| 0.3/-1                 | 0.56/-1        | 0.41/-1        | 0.32/-1        | 4.5/18 | 52  | 113 | 179 | 189 | 19/25.2                              |
| 0.37/0                 | 0.56/-1        | 0.41/-1        | 0.32/1         | 1.4/16 | 65  | 101 | 179 | 189 | 24.5/28.3                            |
| 0.44/+1                | 0.56/-1        | 0.41/-1        | 0.32/-1        | 0/15   | 77  | 90  | 179 | 189 | 27.8/30.4                            |
| 0.44/+1                | 0.70/+1        | 0.41/-1        | 0.32/-1        | 0/13   | 97  | 113 | 122 | 189 | 20.8/23.4                            |
| 0.44/+1                | 0.70/+1        | 0.53/+1        | 0.32/-1        | 0/10   | 125   | 146 | 158 | 150 | 27.8/31.3                            |
| 0.44/+1                | 0.70/+1        | 0.53/+1        | 0.42/+1        | 2.5/10 | 164   | 192 | 207 | 197 | 27.8/31.3                            |
| 0.3/-1                 | 0.7/+1         | 0.53/+1        | 0.42/+1        | 4.9/15 | 112   | 240 | 207 | 197 | 14.6/20.8                            |
| 0.37/0                 | 0.63/0         | 0.47/0         | 0.37/0         | 6.5/18 | 97  | 152 | 199 | 196 | 26/29.8                              |
| 0.44/+1                | 0.56/-1        | 0.53/+1        | 0.32/-1        | 0/10   | 100   | 117 | 231 | 150 | 39.6/41                              |

1. Above the line of the draft of the cone and the strength of concrete without the addition of S-3, and below the line that with the addition of S-3 at  $X_{sp} = 0.02$ . Above the line, the parameters of the composition in physical terms, and below the line—in code. 3.  $X_1 = V_{LKD} / (V_{LKD} + V_{ash})$ ,  $X_2 = (V_{LKD} + V_{ash}) / (V_{LKD} + V_{ash} + V_c)$ ,  $X_3 = (V_{LKD} + V_{ash} + V_c) / (V_{LKD} + V_{ash} + V_c + V_w)$ , and  $X_4 = (V_{LKD} + V_{ash} + V_c + V_w) / (V_{LKD} + V_{ash} + V_w + V_{ag})$ .

components into concrete mixtures makes it possible to increase the strength of concrete by 27%–54%. At the same time, with the consumption of cement up to 200 kg/m<sup>3</sup>, ash 100.150 kg/m<sup>3</sup>, and LKD 50.100 kg/m<sup>3</sup>, it seems possible to obtain concrete with a compressive strength of 20.30 MPa.

Characteristically, the joint introduction of LKD and S-3 has a positive effect on the strength of concrete even at a constant water content, which can be explained by the creation of better conditions for compaction and interparticle interactions in hardening concrete.

Analysis of the steamed concrete strength model shows that the main trends in the influence of the composition of the concrete mixture on the mixed binder remain unchanged. At the same time, the influence of LKD on the strength of concrete after steaming, as

shown by the assessment of the corresponding coefficients of the model, slightly increases. Both in the concrete strength model of normal and steamed concrete, the effect of the  $X_4$  influence, which characterizes the volume concentration of the paste, including, along with cement and ash, a lime–carbonate component, turned out to be insignificant in the chosen range of variation. This result shows that, as in conventional cement concretes, in the studied concretes, not the quantity, but the quality of the matrix, which is characterized by the quantitative ratios of cement, ash, LKD, and water, is of decisive importance within certain limits.

To assess the kinetics of strength increase of cement–ash concretes under normal conditions, the necessary tests were carried out not only in 28 but also in 7, 90, and 180 days. The criterion for the intensity of strength increase was the coefficient

TABLE 7 Intensity of the increase in the concrete strength.

| Composition parameters |       |       |       | Concrete strength increase intensity factors over time, days |    |      |      |
|------------------------|-------|-------|-------|--|----|------|------|
| $X_1$                  | $X_2$ | $X_3$ | $X_4$ | 7  | 28 | 90   | 180  |
| 0.3                    | 0.56  | 0.41  | 0.32  | 0.65   | 1  | 1.12 | 1.20 |
| 0.37                   | 0.56  | 0.41  | 0.32  | 0.67   | 1  | 1.15 | 1.21 |
| 0.44                   | 0.56  | 0.41  | 0.32  | 0.68   | 1  | 1.17 | 1.23 |
| 0.44                   | 0.70  | 0.41  | 0.32  | 0.71   | 1  | 1.18 | 1.24 |
| 0.44                   | 0.70  | 0.53  | 0.32  | 0.71   | 1  | 1.19 | 1.24 |
| 0.44                   | 0.70  | 0.53  | 0.42  | 0.70   | 1  | 1.20 | 1.23 |
| 0.3                    | 0.70  | 0.53  | 0.42  | 0.68   | 1  | 1.18 | 1.22 |
| 0.37                   | 0.63  | 0.47  | 0.37  | 0.71   | 1  | 1.18 | 1.25 |
| 0.44                   | 0.56  | 0.53  | 0.32  | 0.72   | 1  | 1.09 | 1.26 |
| 0                      | 0.56  | 0.41  | 0.32  | 0.61   | 1  | 1.08 | 1.15 |
| 0                      | 0.70  | 0.53  | 0.32  | 0.57   | 1  | 1.10 | 1.17 |

$$X_1 = V_{LKD}/(V_{LKD} + V_{ash}), X_2 = (V_{LKD} + V_{ash})/(V_{LKD} + V_{ash} + V_c), X_3 = (V_{LKD} + V_{ash} + V_c)/(V_{LKD} + V_{ash} + V_c + V_w), \text{ and } X_4 = (V_{LKD} + V_{ash} + V_c + V_w)/(V_{LKD} + V_{ash} + V_w + V_{ag}).$$

$K=R_n/R_{28}$ , where  $n$  is the number of days of hardening. The results of the experiments are given in Table 7.

From the aforementioned data, it can be stated that the introduction of lime kiln dust additive accelerates the hardening of cement–ash concretes, both at an early and at a later age. At the same time, the most noticeable effect of strength growth acceleration is typical for such compositions, where LKD consumption varies within 50.100 kg/m<sup>3</sup>, ash 90.150 kg/m<sup>3</sup>, and cement 120.180 kg/m<sup>3</sup>.

## 4 Conclusion

- 1 The introduction of lime kiln dust (LKD) additives into cement–ash pastes increases the intensity of their hydration. Experimental data show that the catalytic effect of LKD on the hydration of cement–ash pastes is due to the presence of LKD as an oxide, as well as calcium carbonate.
- 2 Analysis of the change in setting time and plastic strength when LKD is introduced into cement–ash pastes shows its active influence on the formation of the coagulation–crystallization structure of cement–ash stone.
- 3 The addition of LKD to cement–ash concrete mixtures contributes to an increase in their water demand, which is leveled by the introduction of a superplasticizer.
- 4 Analysis of the experimental–statistical model of mobility made it possible to establish the influence of the compositional factors of cement–ash concrete mixtures with the addition of LKD and superplasticizer on the value of their cone draft and its change over time, which makes it possible to regulate these parameters in the required area.
- 5 The results of the experiments and the mathematical models of the strength of cement–ash concretes obtained on their basis during normal hardening and steaming indicate a positive effect of the addition of LKD on the compressive strength of concrete in the age from 7 to 180 days.

## Data availability statement

The datasets presented in this study can be found in online repositories. The names of the repository/repositories and accession number(s) can be found in the article/supplementary material.

## Author contributions

Conceptualization: LD and VZ; methodology: LD and VZ; software: VZ; validation: VZ; formal analysis: VZ; investigation: VZ; resources: LD; data curation: VZ; writing—original draft preparation: LD and VZ; writing—review and editing: LD and VZ; visualization: VZ; supervision: LD; project administration: LD; funding acquisition: LD. All authors contributed to the article and approved the submitted version.

## Conflict of interest

The authors declare that the research was conducted in the absence of any commercial or financial relationships that could be construed as a potential conflict of interest.

## Publisher's note

All claims expressed in this article are solely those of the authors and do not necessarily represent those of their affiliated organizations, or those of the publisher, the editors, and the reviewers. Any product that may be evaluated in this article, or claim that may be made by its manufacturer, is not guaranteed or endorsed by the publisher.

## References

- Aquino, C., Inoue, M., Miura, H., Mizuta, M., and Okamoto, T. (2010). The effects of limestone aggregate on concrete properties. *Constr. Build. Mater.* 24, 2363–2368.
- Bandara, N., Hettiarachchi, H., Jensen, E., and Binoy, T. H. (2020). Upcycling potential of industrial waste in soil stabilization: Use of kiln dust and fly ash to improve weak pavement subgrades encountered in Michigan, USA. *Sustainability* 12, 7226. doi:10.3390/su12177226
- Bonavetti, V. L., Rahhal, V. F., and Irassar, E. F. (2001). Studies on the carboaluminate formation in limestone filler-blended cements. *Cem. Concr. Res.* 31, 853–859.
- Box, G. E. P., Hunter, J. S., and Hunter, W. G. (2005). *Statistics for experimenters: Design, discovery, and innovation*. New Jersey: Wiley, 672.
- Cao, M., Ming, X., He, K., Li, L., and Shen, S. (2019). Effect of macro-, micro- and nano-calcium carbonate on properties of cementitious composites—a review. *Materials* 12, 781. doi:10.3390/ma12050781
- CEN (2009). “Testing fresh concrete—Part 2: Slump-test,”. EN 12350-2:2009 (Brussels, Belgium: CEN).
- CEN (2021). “Testing hardened concrete—Part 1: Shape, dimensions and other requirements for specimens and moulds,”. EN 12390-1:2021 (Brussels, Belgium: CEN).
- Cheah, C. B., Tan, L. E., Mahyuddin, R., Bin, M. A., and Kim, H. M. (2022). Properties and microstructure of lime kiln dust activated slag-fly ash mortar. *Constr. Build. Mater.* 347, 128518. doi:10.1016/j.conbuildmat.2022.128518
- Chinnu, S. N., Minnu, S. N., Bahurudeen, A., and Senthilkumar, R. (2021). Recycling of industrial and agricultural wastes as alternative coarse aggregates: A step towards cleaner production of concrete. *Constr. Build. Mater.* 287, 123056. doi:10.1016/j.conbuildmat.2021.123056
- Dvorkin, L., and Dvorkin, O. (2006). *Basic of concrete science: Optimum design of concrete mixtures*. Arlington, Virginia, United States: Kindle Edition, 237.
- Dvorkin, L., Dvorkin, O., and Ribakov, Y. (2012). *Mathematical experiments planning in concrete technology*. New York, NY, USA: Nova Science Publishers, Inc., 173.
- Dvorkin, L., Zhitkovsky, V., Sitarz, M., and Hager, I. (2022). Cement with fly ash and metakaolin blend—drive towards a more sustainable construction. *Energies* 15, 3556. doi:10.3390/en15103556
- Dweck, J., Buchler, P. M., Coelho, A. C. V., and Cartledge, F. K. (2000). Hydration of a Portland cement blended with calcium carbonate. *Thermochim. Acta* 346, 105–113.
- Golewski, G. L. (2023). Mechanical properties and brittleness of concrete made by combined fly ash, silica fume and nanosilica with ordinary Portland cement. *AIMS Mater. Sci.* 10 (3), 390–404. doi:10.3934/mat.2023021
- Hasanbeigi, A., Price, L., and Lin, E. (2012). Emerging energy-efficiency and CO<sub>2</sub> emission-reduction technologies for cement and concrete production: A technical review. *Renew. Sustain. Energy Rev.* 16 (8), 6220–6238.
- Juenger, M. C. G., and Siddique, R. (2015). Recent advances in understanding the role of supplementary cementitious materials in concrete. *Cem. Concr. Res.* 78, 71–80.
- Locher, F. W. (2006). *Cement—principles of production and use*. Germany: Verlag Bau+Technic YmbH: Dusseldorf, 535.
- Mailvaganam, N. P., and Rixom, M. R. (2019). *Chemical admixtures for concrete*. 3rd ed Boca Raton, FL, USA: CRC Press, 456.
- Masimawati, A. L., Sivakumar, N., Hashim, A. R., and Kamal, N. M. (2015). Performance of lime kiln dust as cementitious material. *Procedia Eng.* 125, 780–787. doi:10.1016/j.proeng.2015.11.135
- Matschei, T., Lothenbach, B., and Glasser, F. P. (2007). The role of calcium carbonate in cement hydration. *Cem. Concr. Res.* 37, 551–558.
- Miller, M. M., and M Callaghan, R. (2004). “Lime kiln dust as a potential raw material in portland cement manufacturing,”. Open-File Report, 2004-1336 (Sunrise Valley Drive Reston, VA, United States: USGS Publications Warehouse). <http://pubs.er.usgs.gov/publication/ofr20041>.
- Poppe, A., and De Schutter, G. (2005). Cement hydration in the presence of high filler contents. *Cem. Concr. Res.* 35, 2290–2299.
- Ramachandran, V. S. (1995). *Concrete admixtures handbook: Properties, science and technology*. New Jersey, NJ, USA: Noyes Publications, 1183.
- Wang, D., Shi, C., Farzadnia, N., Shi, Z., Jia, H., and Ou, Z. (2018). A review on use of limestone powder in cement-based materials: Mechanism, hydration and microstructures. *Constr. Build. Mater.* 181, 659–672.
- Wang, L., Zhang, P., and Golewski, G. (2023). Editorial: Fabrication and properties of concrete containing industrial waste. *Front. Mater* 10, 1169715. doi:10.3389/fmats.2023.1169715
- Wang, X. (2018). Analysis of hydration and strength optimization of cement-fly ash-limestone ternary blended concrete. *Constr. Build. Mater.* 166, 130–140.
- Zhang, Y., Yang, B., Gu, X., Han, D., and Wang, Q. (2023). Improving the performance of ultra-high performance concrete containing lithium slag by incorporating limestone powder. *J. Build. Eng.* 72, 106610. doi:10.1016/j.job.2023.106610
- Zhao, D., and Khoshnazar, R. (2021). Hydration and microstructural development of calcined clay cement paste in the presence of calcium-silicate-hydrate (C-S-H) seed. *Cem. Concr. Compos.* 122, 104162.